

Flutter of Thermally Buckled Composite Sandwich Plates

Le-Chung Shiau[1] and Shih-Yao Kuo[2]

Abstract: A high precision high order triangular plate element is developed for the linear flutter analysis of thermally buckled composite sandwich plates. Due to uneven thermal expansion in the two local material directions, the buckling mode of the plate may be shifted from one pattern to another for certain fiber orientation or plate aspect ratio as the aerodynamic pressure is present. This buckle pattern change alters the frequencies and modes of the plate and that in turn changes the flutter coalescent modes. Numerical results show that temperature has a destabilizing effect on the flutter boundary but the aerodynamic pressure has a stabilizing effect on the buckling boundary.

Keyword: Flutter, composite sandwich plate, thermal buckling, buckle pattern change.

1 Introduction

Because of its outstanding bending rigidity, low specific weight, superior isolating qualities, excellent vibration characteristics and good fatigue properties, sandwich construction has been developed and utilized for almost five decades. Recently, sandwich construction has become even more attractive due to the introduction of advanced composite materials for the faces. In the design of sandwich skins for aircraft wings, one important issue is buckling. High-speed aircraft structural panels are subjected not only to aerodynamic loading, but also to aerodynamic heating. The temperature rise may buckle the plate and reduce the load-carrying capacity. Unlike beams or columns, plates can carry an additional load after buckling without failure. In other words, the plates can be used at temperatures higher than the critical buckling temperature. In order to reduce the weight of aircraft, structure are usually permitted to buckle and operated in postbuckling region. In other words, the plates can be used at temperatures higher than the critical buckling temperature. Plate in its buckled state may be expected to survive under dynamic disturbances. This is particularly true for aircraft and space structures, which may depend on the stiffness and dynamic characteristics of the buckled plates with increasing flight speeds.

Panel flutter is a self-excited oscillation of the external skin of a flight vehicle and is due to dynamic instability of inertia, elastic, and aerodynamic forces of the system. An excellent summary of panel flutter was given by Dowell (1970). This type of aeroelastic instability has received much attention in the past 50 years. As a result, their peculiar phenomenon is now reasonably understood for two- and three-dimensional panels made of conventional isotropic materials. But relatively few works have been devoted to the study of flutter characteristics of panels made of composite materials. Ketter (1967) used Ritz method to study flutter of orthotropic panels with various boundary conditions and angle orthotropic. Sawyer (1977) analyzed flutter of general laminated plates using Galerkin's method and the effects of fiber orientation, stacking sequence, anisotropic property, aspect ratio, and flow angularity were discussed in details. Birman and Librescu (1990) used a higher order transverse shear deformation theory to study the effect of transverse shear deformation on flutter-type instability of cross-ply composite flat panels. Comparisons of their results obtained in the framework within the first order transverse shear deformation and classical counterparts were presented and a number of conclusions concerning their range of

[1] Professor, Department of Aeronautics & Astronautics, National Cheng Kung University, Tainan, Taiwan R.O.C.
[2] Former Graduate Student, now as Assistant Professor at Dept. of Flight Service Management, Aletheia Univ., Tainan, Taiwan, R.O.C.

applicability were outlined. Lee and Cho (1991) analyzed supersonic flutter of clamped symmetric composite panels by the finite element method based on the first-order shear deformation theory. They found that the plate aspect ratio, flow direction, and fiber orientation affect greatly the flutter boundaries. Shiau and Chang (1992) made an extensive study of transverse shear effect on panel flutter of laminated plates by finite element method. They pointed out that the transverse shear deformation might have a significant effect on the flutter boundary of thick plates. If the aerodynamic heating is to be considered, Schaeffer and Heard (1965) examined the effect of a parabolic temperature distribution on the flutter behavior of a flat, rectangular, simply supported panel subjected to supersonic flow over one surface. Their results indicated that the nonlinear distribution of temperature may be as important in affecting the flutter behavior as a uniform comprehensive stress state. Yang and Han (1976) used finite element formulation to treat the flutter problem of a semi-infinite panel that is buckled into large deflections due to aerodynamic heating. A relation between the uniform temperature rise and the in-plane compression force in the postbuckling region were used. Later on, a 54 degree-of-freedom, high-order triangular plate finite element was employed to formulate and analyze the supersonic panel flutter problems by Han and Yang (1983). The effect of biaxial mechanical in-plane compressive stress for a simply supported square panel was studied and boundaries among the flat and stable region, dynamically stable buckled region, and the flutter region were found. Xue and Mei (1993) studied the nonlinear flutter response of panels with temperature effects. From the principle of virtual work, the element nonlinear stiffness formulation for a panel under combined thermal and aerodynamic loads was derived. Effects of nonuniform temperature distributions, panel aspect ratios, and boundary conditions on flutter response of rectangular and triangular panels were presented.

Responses of the composite sandwich structures for bending, buckling, and vibration has been analyzed by many authors (Jijan et al. (2004), Li et al. (2005), Sharnappa et al. (2007)). Recently, Shiau and Kuo (2004) developed a higher order triangular-plate element for thermal postbuckling analysis of a composite sandwich plate. Their results show that a "buckle pattern change" phenomenon may occur in the thermal postbuckling region for certain fiber orientation or aspect ratio of the composite sandwich plate. Later on, Shiau and Kuo (2006) extended their investigation to the analysis of free vibration of a thermally buckled composite sandwich plate. They found that the "buckle pattern change" will alter the sequence and change the magnitude of natural frequencies of the plate. In panel flutter analysis, the determination of the occurrence of aeroelastic instability is through the coupling of natural modes of the system. As the "buckle pattern change" changes the natural frequencies and natural modes of the plate, it may have significant effect on the flutter behavior of the composite sandwich plate. In the present study, a high precision high order triangular plate element with shear deformation effect developed in Shiau and Kuo (2006) is extended for the linear flutter analysis of thermally buckled sandwich plates with composite laminated faces and honeycomb cores. The effects of "buckle pattern change", plate aspect ratio, fiber orientation, and temperature on the flutter behavior of the plate are discussed in detail.

2 Formulations

Consider a rectangular composite sandwich plate with length a, width b, and total thickness h. The sandwich panel is assumed to consist of two balanced laminated face sheets of the same thickness f and an orthotropic honeycomb core of thickness c. The face sheets are fabricated with N_f layer orthotropic laminates. Supersonic airflow with air density ρ_∞, flow velocity V_∞, Mach number M_∞, and aerodynamic pressure ΔP is assumed passing over the top surface of the plate. The total transverse displacement of the plate is assumed to be the sum of the displacement due to bending of the plate w_b and that due to shear deformation of the core w_s. Adopting the Von Karman large deflection assumptions, the strain in the plate can be written as

$$\{\varepsilon\} = \{\varepsilon_0\} + z\{\kappa\} + \{\delta\} \tag{1}$$

where $\{\varepsilon_0\}$, $\{\kappa\}$, $\{\delta\}$ are the mid-plane strain, plate curvature, and large deflection strain, respectively.

The stress-strain relation of the sandwich plate subjected to temperature rise ΔT is given by

$$\{\sigma\}_k = \left[\overline{Q}\right]_k (\{\varepsilon\} - \Delta T\{\alpha\}_k) \tag{2a}$$

$$\{\tau\} = \left[\overline{Q}\right]\{\gamma\} \tag{2b}$$

where $\overline{Q}_{ij}$ are the transformed reduced stiffness.

For sandwich plate having honeycomb core, it is reasonable to assume that the transverse normal stiffness of the core is infinitely large and the core makes no contribution to the bending and membrane stiffness of the sandwich plate. But the shear strains in the core of the sandwich need to be considered due to a low transverse modulus of rigidity of the core. The force and moment resultants of the sandwich plate are then defined as

$$\{N\} = [A]\left\{\varepsilon^0\right\} + [A]\{\delta\} - \left\{N^{\Delta T}\right\} \tag{3a}$$

$$\{M\} = [D]\{\kappa\} \tag{3b}$$

$$\{V\} = [S]\{\gamma\} \tag{3c}$$

where the extensional stiffness $[A]$, bending stiffness $[D]$ of the panel, and transverse shear stiffness $[S]$ are the usual composite terms.

The thermal forces $\left\{N^{\Delta T}\right\}$ induced by the temperature change are defined as

$$\left\{N^{\Delta T}\right\} = 2T_u \sum_{k=1}^{N_f} \left[\overline{Q}\right]_k \{\alpha\}_k (h_k - h_{k-1}) \tag{4}$$

The total strain energy can be expressed as

$$\begin{aligned} U = &\frac{1}{2}\int_A \{\varepsilon_0\}^T [A]\{\varepsilon_0\}\, dA \\ &+ \frac{1}{2}\int_A \{\kappa\}^T [D]\{\kappa\}\, dA \\ &+ \frac{1}{2}\int_A \left(\{\delta\}^T [A]\{\varepsilon_0\} + \{\varepsilon_0\}^T [A]\{\delta\}\right) dA \\ &+ \frac{1}{2}\int_A \{\delta\}^T [A]\{\delta\}\, dA \\ &+ \frac{1}{2}\int_A \{\gamma\}^T [S]\{\gamma\}\, dA \\ &- \frac{1}{2}\int_A \left(\{\delta\}^T\left\{N^{\Delta T}\right\} + \{\varepsilon_0\}^T\left\{N^{\Delta T}\right\}\right) dA \end{aligned} \tag{5a}$$

The kinematic energy may be expressed as

$$T = \frac{\rho_t h}{2}\int \left(\dot{w}_b^2 + 2\dot{w}_b\dot{w}_s + \dot{w}_s^2\right) dA \tag{5b}$$

where $\rho_t h = 2\rho_f f + \rho_c c$.

The work done by the non-conservative aerodynamic loading may be expressed as

$$W_{nc} = \int \Delta p\,(w_b + w_s)\, dA \tag{5c}$$

For high supersonic Mach numbers ($M_\infty > 1.6$), the aerodynamic pressure loading is assumed to follow quasi-steady aerodynamic theory:

$$\Delta P = -\frac{\rho_\infty V_\infty^2}{\sqrt{M_\infty^2 - 1}} \cdot \left((w_{b,x} + w_{s,x}) + \frac{M_\infty^2 - 2}{M_\infty^2 - 1}\frac{1}{V_\infty}(\dot{w}_b + \dot{w}_s)\right) \tag{6}$$

The work done by the non-conservative aerodynamic loading may be divided into two parts: aerodynamic force part and aerodynamic damping part as

$$W_{nc} = W_a + W_d \tag{7}$$

where

$$W_a = -\frac{\rho_\infty V_\infty^2}{\sqrt{M_\infty^2 - 1}}\int (w_{b,x} + w_{s,x})(w_b + w_s)\, dA$$

$$W_d = -\frac{\rho_\infty V_\infty^2 (M_\infty^2 - 2)}{(M_\infty^2 - 1)^{3/2}}\int (\dot{w}_b + \dot{w}_s)(w_b + w_s)\, dA$$

2.1 Finite Element Formulation

Consider a triangular element with thickness h as shown in Fig. 1. The total transverse displacement of the plate is assumed to be the sum of the displacement due to bending of the plate and that due to shear deformation of the core. For simplicity, the four displacement functions for the in-plane, bending and shear deformation are assumed to have the same form. These displacement functions for u, v, w_b, and w_s can be expressed in the local $\xi - \eta$ coordinate system as a

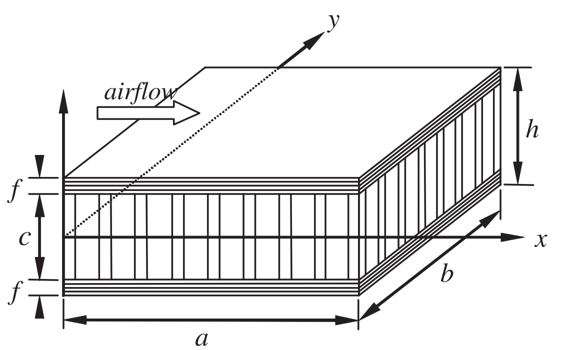

Figure 1: Geometry of a composite sandwich panel

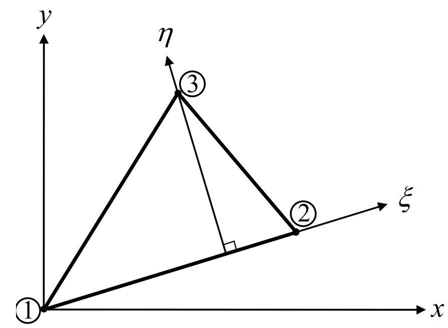

Figure 2: Global/local coordinate systems for a triangular plate element.

polynomial to the complete fifth order of ξ and η, excluding the term $\xi^4\eta$. Omitting the term $\xi^4\eta$ is to ensure that the slope normal to the edge $\eta = 0$ varies cubically along ξ, so that the normal slope compatibility along this edge is satisfied:

$$u = \sum_{i=1}^{20} \alpha_i \xi^{m_i} \eta^{n_i}; \qquad v = \sum_{i=1}^{20} \beta_i \xi^{m_i} \eta^{n_i}; \tag{8a}$$

$$w_b = \sum_{i=1}^{20} \gamma_i \xi^{m_i} \eta^{n_i}; \quad w_s = \sum_{i=1}^{20} \zeta_i \xi^{m_i} \eta^{n_i} \tag{8b}$$

where m_i = (0, 1, 0, 2, 1, 0, 3, 2, 1, 0, 4, 3, 2, 1, 0, 5, 3, 2, 1, 0), n_i = (0, 0, 1, 0, 1, 2, 0, 1, 2, 3, 0, 1, 2, 3, 4, 0, 2, 3, 4, 5), and α_i, β_i, γ_i, ζ_i are constants to be determined by using conditions at nodal point.

Substituting the displacement functions in Eqs. (8) into Eq. (5) and integrating over the plate element, the strain energy of an element can be expressed as

$$U_e = \frac{1}{2}\{q\}^T \left([k] + \frac{1}{3}[n_1] + \frac{1}{6}[n_2]\right)\{q\} \tag{9a}$$

$$U_{\Delta T} = -\frac{1}{2}\Delta T\left[\{q\}^T\left[k_N^{\Delta T}\right]\{qt\} + \{q\}^T\left\{f^{\Delta T}\right\}\right] \tag{9b}$$

$$T = \frac{1}{2}\left\{\frac{\partial q}{\partial t}\right\}^T [m]\left\{\frac{\partial q}{\partial t}\right\} \tag{9c}$$

$$W_a = \frac{\rho_\infty V_\infty^2}{\sqrt{M_\infty^2 - 1}}\{q\}^T[a]\{q\} \tag{9d}$$

$$W_d = \frac{\rho_\infty V_\infty^2 (M_\infty^2 - 2)}{(M_\infty^2 - 1)^{3/2}}\{q\}^T[c]\{\dot{q}\} \tag{9e}$$

where $[k]$, $[n_1]$, $[n_2]$ are the element linear, first-order, second-order nonlinear stiffness matrices, $\left[k_N^{\Delta T}\right]$ is the geometrical stiffness matrix due to uniform thermal load, $\left\{f^{\Delta T}\right\}$ is the thermal loading vector due to temperature gradient, $[m]$ is the mass matrix, $[a]$ is the element aerodynamic matrix, $[c]$ is the aerodynamic damping matrix, and $\{q\}$ contains all the nodal degree of freedoms.

On assembling all element matrices and load vectors and then applying suitable boundary conditions, and introducing the following non-dimensional parameters and constants

$$\lambda = \frac{\rho_\infty V_\infty^2}{\sqrt{M_\infty^2 - 1}}\frac{a^3}{D_{11}^0}, \qquad \mu = \frac{\rho_\infty a}{\rho_t h}, \qquad g = \frac{\mu}{M_\infty},$$

$$D_{11}^0 = \frac{E_1^2\left(h^3 - c^3\right)}{12\left(E_1 - \nu_{12}^2 E_2\right)}, \; \omega_0 = \sqrt{\frac{D_{11}^0}{\rho_t h a^4}}, \; \tau = \omega_0 t$$

The governing equation in matrix form for the nonlinear flutter analysis of thermal buckled composite sandwich plate is obtained as

$$\frac{1}{\rho_t h}[M]\{\ddot{Q}\} + \sqrt{\lambda g}[C]\{\dot{Q}\} + \left[\frac{a^4}{D_{11}^0}\left([K] + \frac{1}{2}[N_1] + \frac{1}{3}[N_2] - \Delta T\left[K_N^{\Delta T}\right]\right) + \lambda a[A]\right]\{Q\} = \frac{\Delta T a^4}{D_{11}^0}\left\{F^{\Delta T}\right\} \quad (10)$$

where $\{Q\}$ is the global nodal degree of freedoms vector for the assembled structure.

Let the total response of the plate to be the sum of displacement due to static deformation and that due to dynamic deformation as

$$\{Q\} = \{Q_s\} + \{Q_d\} = \{Q_s\} + \{\phi\}e^{i\omega\tau} \quad (11)$$

where $\{\phi\}$ is the mode shape vector. By substituting above equation into Eq. (10) and neglecting the higher order terms related to $\{Q_d\}$, i.e., considered for small amplitude vibration, then Eq. (10) can be written into two sets of equations as

$$\left([K] + \frac{1}{2}[N_1] + \frac{1}{3}[N_2] - \Delta T\left[K_N^{\Delta T}\right] + \lambda\frac{D_{11}^0}{a^3}[A]\right)\{Q_s\} = \Delta T\left\{F^{\Delta T}\right\} \quad (12a)$$

$$\left(-\kappa_a\omega_0^2[M] + [K] + [N_1] + [N_2] - \Delta T\left[K_N^{\Delta T}\right] + \lambda\frac{D_{11}^0}{a^3}[A]\right)\{Q_d\} = \{0\} \quad (12b)$$

Eq. (12a) is a set of nonlinear algebraic equations that yields the static deflection of the thermally buckled plate under the influence of aerodynamic pressure and aerodynamic heating. Eq. (12b) is a set of linear equations to determine the flutter boundary of the thermally buckled plate. For a nontrivial solution to exist, the determinant of the matrices in parentheses of Eq. (12b) must equal to zero, which gives the characteristic equation for the eigenvalue. Eq. (12b) can be solved in frequency domain by assuming that the plate motion is represented by an exponential function of time as in Eq. (11). The two governing equations may be rewritten as

$$\left([K_N] + \lambda\frac{D_{11}^0}{a^3}[A]\right)\{Q_s\} = \Delta T\left\{F^{\Delta T}\right\} \quad (13a)$$

$$\left|-\kappa_a\omega_0^2[M] + [K_T] + \lambda\frac{D_{11}^0}{a^3}[A]\right| = 0 \quad (13b)$$

where $[K_T]$ is the tangent stiffness matrix. The nonlinear equation in Eq. (13a), which governing the thermal postbuckling behavior of composite sandwich plate, is a static algebraic equation that can be solved by Newton-Raphson method. After the equilibrium state of thermal postbuckling analysis is obtained, the nonlinear tangent stiffness matrix $[K_T]$ in Eq. (13b) can be obtained. Thus, Eq. (13b) becomes standard eigenvalue problem and is applied to study the linear flutter of thermally buckled composite sandwich plates.

3 Numerical Results

In the following, a simply supported rectangular composite sandwich plate consisting of graphite epoxy laminated face sheets and aluminum honeycomb core is analyzed. The material properties for the graphite epoxy laminated face sheets are E_1 = 181 Gpa, E_2 = 10.3 Gpa, G_{12} = 7.17 Gpa, $\nu_{12} = 0.28$, $\alpha_1 = 0.02 \times 10^{-6}/^oC$, $\alpha_2 = 22.5 \times 10^{-6}/^oC$, $\rho_f = 1.6 \times 10^3 Kg/m^3$. The material property for the aluminum honeycomb core is $\rho_c = 1.6 \times 10^1 Kg/m^3$, G_{23C} = G_{31C}= 0.14 Gpa. The thicknesses of each face and the core are 0.5mm and 10mm, respectively. Two different stacking sequences of the plate are considered: (1) [(0/90)$_2$/core]$_s$ sandwich plate and (2) [($\pm\theta$)$_2$/core]$_s$ sandwich plate.

3.1 [(0/90)$_2$/core]$_s$ cross-ply laminated sandwich plates

For linear flutter, the plate motion can be divided into three types: (1) plate remains stable and flat; (2) plate buckles but is dynamically stable; (3) flutter occurs (either limit-cycle oscillation or chaotic motion). Figure 3 shows the stability boundaries between these three types of motion for rectangular [(0/90)$_2$/core]$_s$ sandwich plates with two different aspect ratios. It is seen that temperature has a destabilizing effect on the flutter boundary (line *AC*) when the plate remains in flat and stable condition. But when the plate is in buckled but dynamically stable condition, temperature will raise the flutter boundary (line *CD*). On the other hand, due to stabilizing effect of the aerodynamic pressure, the critical buckling temperature of the plate will be higher when the aerodynamic pressure is present (line *BC*).

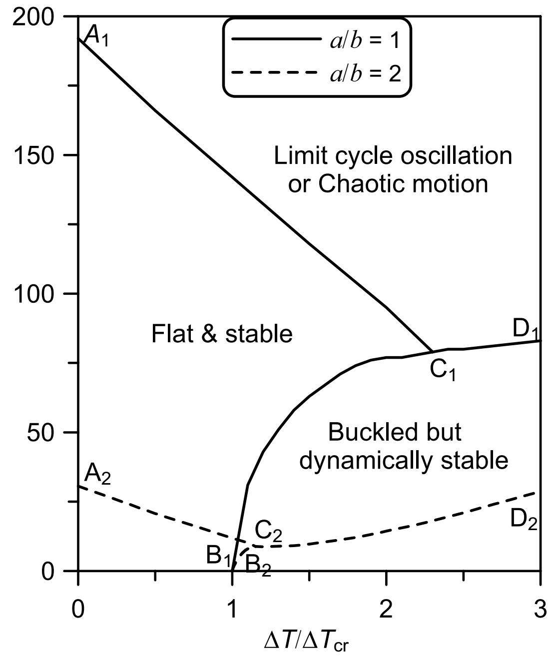

Figure 3: Stability boundaries for rectangular $[(0/90)_2/\text{core}]_s$ sandwich plate

Flutter occurs through the coupling of two modes of the plate. Figure 4 shows the flutter coalescence plot of the square $[(0/90)_2/\text{core}]_s$ plate discussed in Fig. 3 with three different temperatures. For $\lambda = 0$ the eigenvalues of all modes of the plate are purely real. As λ increases from zero, the eigenvalues of two modes approach each other and coalesce at a critical value of λ, called λ_{cr}, where flutter occurs. For all the three temperature cases, the coalescent pair is the first and the second modes of the plate. For the $\Delta T/\Delta T_{cr} = 2$ case, the plate goes through three motion types. As the aerodynamic pressure starts from zero, the plate is in its buckled but dynamically stable condition due to the temperature higher than the buckling temperature. As λ increases to the boundary line *BC* in Fig. 2, one of the eigenvalues will drop to zero. At this moment ($\lambda = 77$), plate goes into flat and stable condition and remains in that condition until λ further increases to 96 where two modes coalesce and flutter occurs.

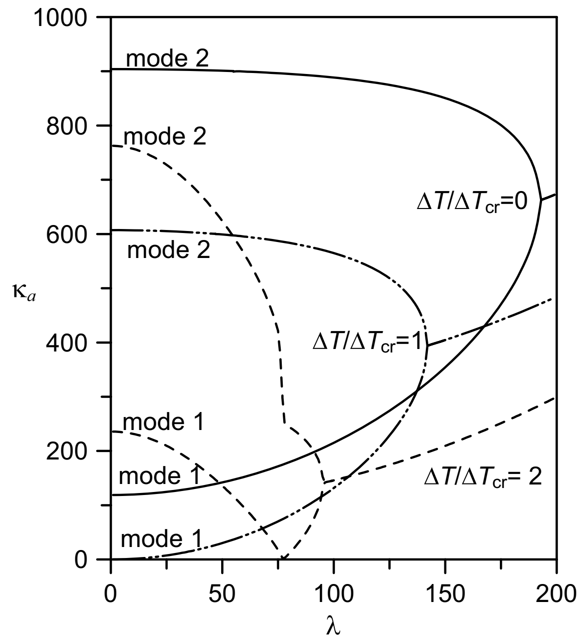

Figure 4: Flutter coalescence plot of square $[(0/90)_2/\text{core}]_s$ sandwich plates

The foregoing phenomenon may also be explained by the contour plot of the two modal shapes at various λ shown in Fig. 5 for the $\Delta T/\Delta T_{cr} = 2$ case. At $\lambda = 0$, the two natural modes of the buckled plate are modes 1 and 2. The shapes of the two modes are gradually changed with the increase of aerodynamic pressure, especially in the flow direction. Finally, these two modes coalesce into a single flutter mode when λ reaches λ_{cr}.

3.2 $[(\pm\theta)_2/\text{core}]_s$ angle-ply laminated sandwich plates

Figure 6 depicts the map in λ and $\Delta T/\Delta T_{cr}$ space which identifies the flutter boundaries for a simply supported square $[(\pm 30)_2/\text{core}]_s$ sandwich plate. Here, a phenomenon called “buckle pattern change” occurs in the postbuckling region when aerodynamic pressure is present. The

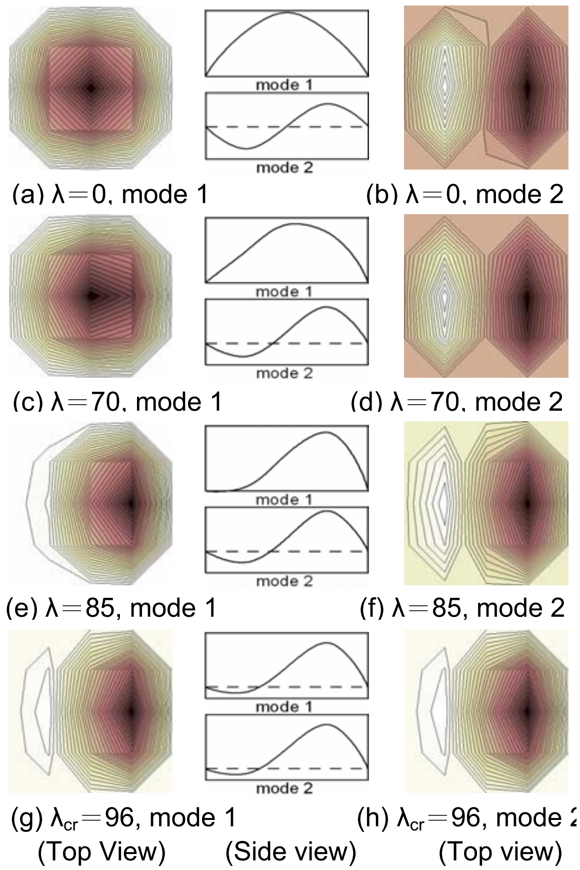

Figure 5: Contour plot of static deflection for square [(0/90)$_2$/core]$_s$ sandwich plate at $\Delta T/\Delta T_{cr}$=2

buckle pattern change occurred in the postbuckling region means the buckling shape of the plate will shift from one buckling mode to another as λ increases. This shifting will alter the flutter frequencies and modes of the plate and that in turn changes the flutter coalescence pair. This phenomenon can also be seen in the flutter coalescence plot shown in Fig. 7 for the [$(\pm 30)_2$/core]$_s$ sandwich plate with $\Delta T/\Delta T_{cr}$ = 3. As the flutter speed increases from zero, all frequencies of the plate will decrease with the increase of λ. At λ = 78, the frequency of square sandwich plate mode 1 drops to zero and the plate goes through the first buckle pattern change phenomenon. At this moment, the frequencies of all modes have a sudden upward jumping and then decrease again as the flutter speed increases further. When the flutter speed reaches a value of 330, buckle pattern change occurs again and the frequency of mode 3 drops to zero. After this point, two modes of the plate coalesce at λ_{cr} = 382.

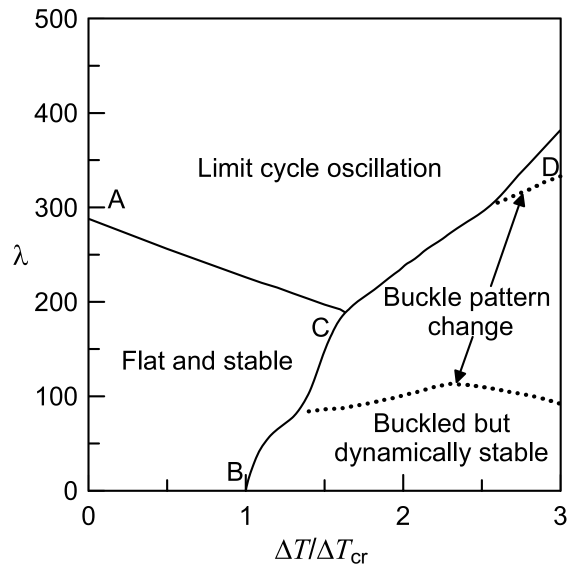

Figure 6: Flutter boundaries for [$(\pm 30)_2$/core]$_s$

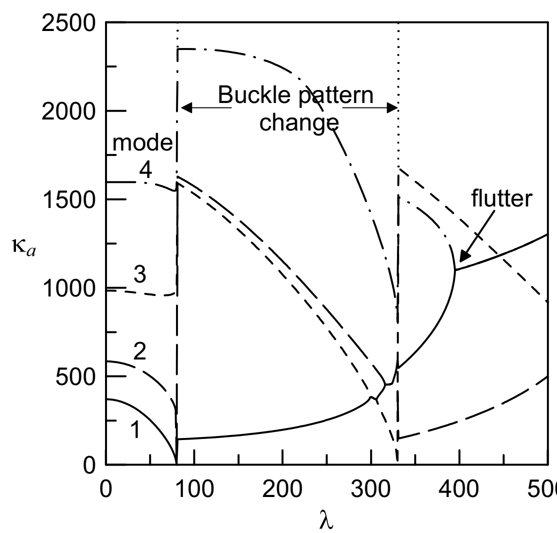

Figure 7: Flutter coalescence plot of [$(\pm 30)_2$/core]$_s$ sandwich plate ($\Delta T/\Delta T_{cr}$= 3)

Figure 8 displays the effect of fiber angle on the flutter boundaries for a square [$(\pm\theta)_2$/core]$_s$ sandwich plate with four different temperatures.

For the $\Delta T/\Delta T_{cr}$ = 0 and $\Delta T/\Delta T_{cr}$ = 1 cases, rotating fiber away from x-axis will reduce the stiffness of the plate in the x-direction which in turn lower the flutter boundary of the plate. When the plate is in its buckling stage, that is the $\Delta T/\Delta T_{cr}$ = 1 case, the flutter boundary is reduced significantly when the fiber is orientated at an angle between 65° and 90°. For the $\Delta T/\Delta T_{cr}$ = 2 and $\Delta T/\Delta T_{cr}$ = 3 cases, general trends are the same as that of the other two cases except for the plate with fiber orientated between 0° and 30°. For plate with those fiber orientations, rotating fiber away from x-axis may raise the flutter boundary of the plate. It is seen that when the fiber angle is between 0° and 20°, the flutter boundary is raising with the fiber angle. But when the fiber angle varies from 20° to 30°, the flutter boundary is drop sharply. The reason to cause this variation is due to the "buckle pattern change" phenomenon and the effect of this phenomenon on the flutter boundary variation can be clearly seen from flutter coalescence plot. Figure 9 shows the flutter coalescence plots of the square angle-ply laminated sandwich plate with fiber angle varied from 0° to 30° for the case of $\Delta T/\Delta T_{cr}$ = 2. First, for the plate with fiber angle less than 20°, there is only one occurrence of "buckle pattern change" before the flutter begins. The "buckle pattern change" is occurred at λ = 163 for θ = 0° and the occurrence point is gradually shifted to λ = 180, 204, and 238 for θ = 10°, 15°, and 20°, respectively. Because of the "buckle pattern change" and the shifting of the occurrence point, the flutter boundary of the plate is raising with the fiber angle. Second, for the plate with fiber angle larger than 20°, there are two occurrences of "buckle pattern change" before the flutter begins. Due to the second "buckle pattern change", the frequencies of the plate are dropped sharply, that is these frequencies are closer to each other. Once the frequencies of two coalescent modes are close to each other, they will coalesce to a lower value of λ.

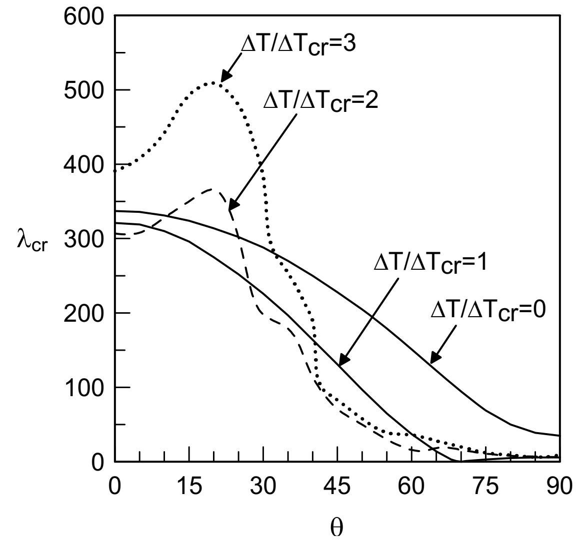

Figure 8: Flutter boundary vs. fiber angle for square $[(\pm\theta)_2/\text{core}]_s$ sandwich plates

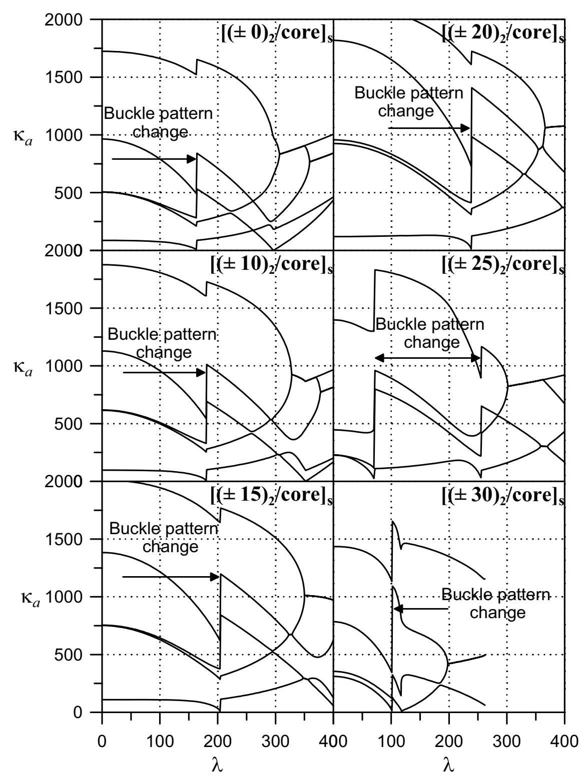

Figure 9: Flutter coalescence plot of square angle-ply composite sandwich plates

4 Conclusions

The linear flutter of a thermally buckled composite sandwich plate is presented. Based on the present results, the following conclusions can be drawn:

(1) Temperature has a destabilizing effect on the

flutter boundary but the aerodynamic pressure has a stabilizing effect on the buckling boundary.

(2) Buckle pattern change occurred in the post-buckling region alters the frequencies and modes of the plate and that in turn changes the flutter coalescent modes.

(3) The frequency coalescence usually occurs between the first two modes. However, if there is buckle pattern change occurred in the post-buckling region, the coalescent pair may be between higher modes.

Acknowledgement: This work was supported by the NSC of the Republic of China through Grants no. NSC 92-2212-E-006-094.

References

Birman, V.; Librescu, L. (1990): Supersonic flutter of shear deformable laminated composite flat panels. *Journal of Sound and Vibration*, Vol. 139, pp. 265–275.

Dowell, E. H. (1970): Panel Flutter: A review of the aeroelastic stability of plates and shells. *AIAA Journal*, Vol. 8, No. 3, pp. 385–399.

Han, A. D.; Yang, T. Y. (1983): Nonlinear panel flutter using high-order triangular finite elements. *AIAA Journal*, Vol. 21, No. 10, pp. 1453–1461.

Jihan, K.; Yong, H. K.; Sung, W. L. (2004): Asymptotic postbuackling analysis of composite and sandwich structures via the assumed strain solid shell element formulation. *CMES: Computer Modeling in Engineering & Sciences.* Vol. 6, No. 3, pp. 263-276.

Ketter, D. J. (1967): flutter of flat, rectangular, orthotropic panels. *AIAA Journal*, Vol. 5, No. 1, pp. 116–124.

Lee, I.; Cho, M. H. (1991): Supersonic flutter analysis of clamped symmetric composite panels using shear deformable finite elements. *AIAA Journal*, Vol. 29, No. 5, pp. 782–783.

Li, J.; Xiang, Z. H.; Xue, M. D. (2005): Three dimensional finite element analysis of honeycomb sandwich composite shells with cutouts. *CMC: Computers, Materials & Continua* Vol. 2, No. 1, pp. 139–150.

Sawyer, J. W. (1977): Flutter and buckling of general laminated plates. *Journal of Aircraft*, Vol. 14, No. 4, pp. 387–393.

Schaeffer, H. G.; Heard, W. L., Jr. (1965): Flutter of a flat panel subjected to a nonlinear temperature distribution. *AIAA Journal*, Vol. 3, No. 10, pp. 1918–1923.

Sharnappa; Ganesan, N.; Sethuraman, R. (2007): Buckling and Free Vibrations of Sandwich General shells of Revolution with Composite facings and Viscoelastic core under Thermal Environment using Semi-analytical Method. *CMES: Computer Modeling in Engineering & Sciences.* Vol. 18, No. 2, pp. 121-144.

Shiau, L. C.; Chang, J. T. (1992): Transverse shear effect on flutter of composite panels. *Journal of Aerospace Engineering, ASCE*, Vol. 5, pp. 465–479.

Shiau, L. C.; Kuo, S. Y. (2004): Thermal post-buckling behavior of composite sandwich plates. *Journal of Engineering Mechanics, ASCE*, Vol. 130, No. 10, pp. 1160–1167.

Shiau, L. C.; Kuo, S. Y. (2006): Free vibration of thermally buckled composite sandwich plates. *Journal of Vibration and Acoustics, ASME*, Vol. 128, No. 1, pp. 1–7.

Xue, D. Y.; Mei, C. (1993): Finite element nonlinear panel flutter with arbitrary temperatures in supersonic flow. *AIAA Journal*, Vol. 31, No. 1, pp. 154–162.

Yang, T. Y.; Han, A. D. (1976): Flutter of thermally buckled finite element panels. *AIAA Journal*, Vol. 14, No. 7, pp. 975–977.